Light Metals 2013 *Edited by: Barry Sadler*
TMS (The Minerals, Metals & Materials Society), 2013

MECHANICAL BEHAVIOUR OF COLD FORMED METAL-POLYMER LAMINATE AND THE INTERACTION OF ITS LAYERS

Feidhlim Ó Dubhlaing[1], David J. Browne[1], Robin Rennicks[2], Connor Rennicks[2]
[1]School of Mechanical and Materials Engineering, University College Dublin, Belfield, Dublin 4, Ireland
[2]Prodieco Ltd, Unit 30, Cookstown Industrial Estate, Tallaght, Dublin 24, Ireland

Keywords: Metal-Polymer Laminate, Tensile, Erichsen, AA8079

Abstract

This research is aimed at characterising and comparing the mechanical properties of a polymer/metal/polymer laminate and its individual layers. The laminate is cold deep drawn for pharmaceutical packaging, thus the properties were characterised at room temperature. The investigation was needed to understand how the layers contribute to formability in terms of elastic and plastic deformation. Particular attention was given to how the properties of the aluminium alloy layer were enhanced by the addition of each polymer layer. Tensile tests were carried out to determine material strengths, anisotropy and strain-hardening. These properties vary for each layer and the dominating properties in the complete laminate are of strong interest. Cup forming tests were performed to establish the forming depth of the constituent layers, carried out in line with the Erichsen cupping test. Wrinkling of the specimen during these cup forming tests had to be avoided, placing strong emphasis on understanding the stretching mechanism.

Introduction

The metal-polymer laminate under investigation in this study is illustrated in Figure 1 and is a PA (Polyamide 6) – Aluminium (AA8079) – PVC (Rigid Polyvinyl Chloride) laminate with layer thicknesses of 25, 47 and 60 microns respectively. The three layers are bonded using appropriate adhesives and primers to prevent delamination during packaging production and its shelf-life. Each layer of the laminate contributes in its own way to the formability of the laminate during cold forming by punch and die tooling. To understand fully the mechanical properties and formability of the laminate, it is necessary to evaluate the limits of formability of each of the layers. Tensile testing of the layers and the laminate allow for the determination of these properties and how the layers may interact. Uniaxial testing of materials does not necessarily indicate the limit of formability in multiaxial deep drawing operations however, so the limit of formability was determined using a punch and die also.

To aid in the determination of the properties, the various attributes of the layers that contribute to or are detrimental to the formability are discussed. Such effects as the water absorptivity of polyamide, the aging or strain-hardening effects of PVC or the annealing of the AA8079 aluminium alloy are quantified. The storage and handling history of the layers is unknown and thus these effects cannot be accounted for, but by comparing and contrasting results in relation to work previously carried out the formability of the laminate can be reasonably determined.

Theory

The aluminium layer in the laminate provides the barrier properties necessary to protect the pharmaceutical product being packaged, and the specific alloy is chosen for its high formability. However this formability is not comparable to that of polymers [1], [2]. The addition of the polyamide layer provides greater elasticity to the aluminium, while the PVC provides rigidity to the formed part and aids in preventing springback [3]. The metal-polymer laminate exhibits mechanical properties that are superior to a metal sheet of equivalent thickness meaning lower forming forces needed during part production.

To avoid both bending and extension forces being induced during and after forming the laminate, symmetry of the laminate properties and geometry is usually created about the middle layer. In some cases, unsymmetrical laminates in terms of geometry and/or properties are produced to meet a given need [4]. It is therefore of great interest to establish the formability of the laminate and its individual layers, with an understanding of the laminate failure in terms of the failure of the laminae [4], [5].

As an example, the mechanical properties of a fibre-metal laminate are observed to display the plasticity of the metal sheet under tensile loading but with a much higher strain-to-failure created by the fibres than would be observed for the metal on its own [6]. In the consideration of laminates it is assumed that the individual laminae are perfectly bonded and that the adhesives and primer layer thicknesses are negligible, discounting the occurrence of shearing in these regions [4].

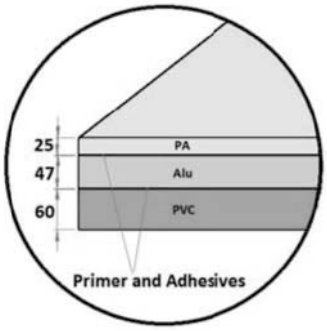

Figure 1 PA6-AA8079-Rigid PVC laminate, with respective thicknesses in microns

Layers

In a complete study of the mechanical properties of this laminate it is necessary to understand the mechanical properties of each layer and how they change with forming environment or pre-treatments.

Polyamide 6, while increasing the elasticity of the aluminium layer, also has high strength, excellent corrosion resistance, good wear resistance and self-lubricating properties [7], all of which are advantageous for cold formed pharmaceutical packaging. The disadvantage of PA6 is that it has a high water absorption rate, and the mechanical properties of the polyamide change with water content. Previous work has been carried out on

this [6], where accelerated conditions were used to determine the water absorptivity of the polymer and the resulting change in mechanical properties tested. An increase in water content did not affect the yield strength to a great degree, with the yield strength measured in the region of 44MPa, but the strain at fracture was reduced by 55.1% in the water-absorbed samples [7]. This indicates that the formability of the laminate is highly dependent on the production, transport and storage environments, particularly with respect to the humidity of the environments.

PVC on the other hand has no noticeable water absorptivity but it exhibits yield and necking phenomena typical of tough thermoplastics [8]. Its stress-strain curve is similar to that for a metallic material but the transition between elastic and plastic deformation includes upper and lower yield strengths between which strain softening occurs, similar to that in Figure 2 [9]. Once the upper yield strength is reached shear bands form resulting in neck initiation, which leads to varying levels of stress and strain across the specimen being loaded [8]. The stress-strain curve determined from testing the polymer may not then truthfully represent the behavior of the polymer due to the varying stress levels across the neck and other sections of the specimen [10]. This neck then has a tendency to propagate through the specimen until it has completely necked [10].

It has been found that the necking behavior of PVC can be controlled by the thermal pre-treatment of the polymer, in terms of either quenching or annealing [8][11], [12]. The curves in Figure 2, representative of illustrations in [9], are examples of pre-treatment effects. Quenching the PVC in iced water for example could eliminate a stress overshoot and strain softening, but as time elapses and the PVC ages, it will return to its original structure and a stress overshoot will result [8]. This increase in yield stress can exceed 10% if the PVC is annealed, with a combination of previous studies indicating an increase from 38MPa for quenched PVC to approximately 50MPa for commercial PVC [11]. As is evident in Figure 2 however, the post yield behavior of the PVC such as flow stress and strain hardening is irrespective of the thermal pre-treatment [9], [11].

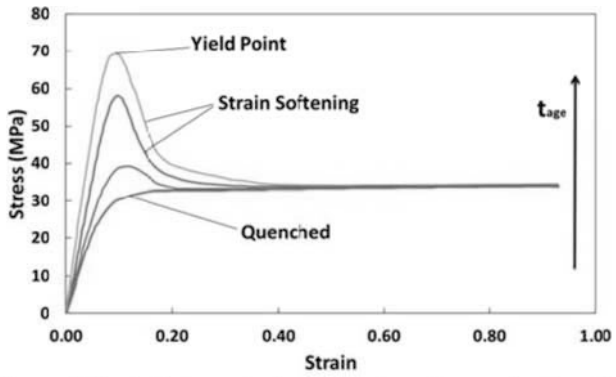

Figure 2 Typical stress-strain curves for a thermoplastic with yielding and subsequent strain softening, and effect of heat treatment on the PVC stress-strain curve

Similar to the heat treatment of PVC, the strain rate has an influence on the stress-strain curve and the eventual fracture of the polymer [13]. Three different ranges for strain rate have been proposed, with differing stress-strain curves and failure mechanisms associated with each. It is deemed that below a strain rate ($\dot{\varepsilon}$) of $1h^{-1}$ ($\sim 0.0003s^{-1}$) uniform deformation of PVC can be induced with minimal stress overshoot, while above this necking occurs at yield [8]. This necking, caused by highly localised levels of strain [13], can then lead to thermal rupture of the neck at sufficiently high $\dot{\varepsilon}$, thought to be greater than $100h^{-1}$ ($\sim 0.03s^{-1}$) [8]. The thermal fracture is as a result of a localised increase in heat in the neck not having sufficient time to dissipate [8], [12].

Another aspect of the plastic deformation of PVC and that can be observed throughout the duration of material testing and forming, is the stress whitening of the polymer. The polymer becomes opaque as it deforms, due to the formation of microvoids throughout the material [13]. The dimensions of these microvoids are on the same scale as the wavelength of light and thus change the refractive index of the polymer. It must be taken into account that this change is more a visual alteration than a change in properties, as the stress-whitened PVC can withstand much the same load as PVC absent of microvoids [13]. This stress whitening occurs once the polymer begins to yield and the polymer chains begin to reorient. A stress 'plateau' is observed during plastic deformation then during which the polymer chains begin to align, but once a significant amount of alignment is achieved and thermal fracture is avoided, strain hardening of the polymer occurs [9], [13].

Aluminium, like many metallic materials, does not display this type of yield and necking phenomena, rather once yielding occurs the material will tend to deform uniformly while strain hardening develops. Once the metal reaches its tensile strength it may then neck [13], but necking is usually negligible [6]. The AA8079 alloy used in this case is extensively used in the packaging industry as a whole [14], due to its excellent elongation at failure and tensile strength versus other available alloys [3]. The alloy is an Al-Fe-Si ternary alloy, amongst other elements in minor proportions [14], and ASTM B479 outlines the acceptable percentage of each alloying element as in Table 1 [15]. Examining the elements present in the alloy it has been observed that the presence of an Mg solute has detrimental effects on the speed at which the alloy can be formed, while the presence of Si atoms increases this speed. This is due to the negative heat of formation between Mg and Al creating immovable clusters that restrict grain boundary sliding, while the Si atoms weaken the aluminium bonds promoting grain boundary sliding [14].

Table I AA8079 alloy composition (%) [15]

Si+Fe	Cu	Mn	Mg	Zn	Ti	Other	Other	Al
1.8	0.2	0.1	0.05	0.1	0.08	0.05 each	0.15 total	98 min

In forming parts from this alloy in its annealed state its formability can be taken full advantage of, with the annealing temperature also playing a role in this formability [14], [16]. The effects of annealing are graphed in Figure 3, determined from previous work [16]. If low temperature annealing is carried out, a decrease in the ductility of the alloy is observed due to the removal of dislocations [16], but at higher annealing temperatures greater control over recrystallisation takes place increasing the deformation potential of the alloy [17]. The necking behavior is also dependent on annealing with a localized neck occurring in the low-temperature annealed state and more diffuse necking in the high-temperature annealed state [16], [17].

Through higher temperature annealing greater control can be obtained on the grain size in the alloy. A differential grain size across a section of material causes non-uniformities in the flow stress of the material [18], whereas a fine, uniform grain size is preferred for sheet metal forming [19]. An ASTM grain size of

7 or finer is sought, which corresponds to a grain diameter of 31.8μm for a uniform, randomly oriented, equiaxed structure [19], [20]. The relative size of the grains compared to the sheet thickness may have an effect on the bulk properties of the material [21], [22], as illustrated in Figure 4, similar to that in previous studies [14].

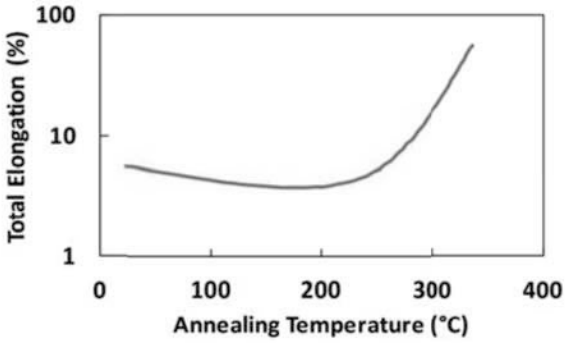

Figure 3 Effect of annealing temperature on the ductility of AA8079

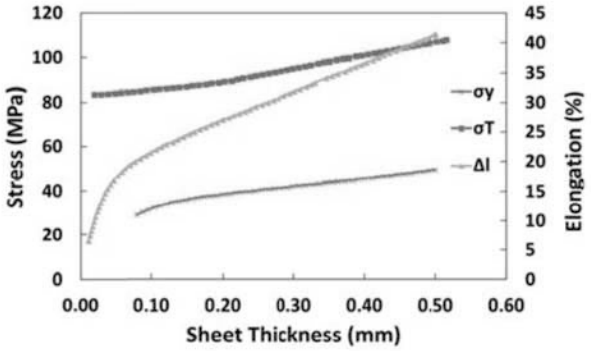

Figure 4 Plasticity (Δl), yield strength (σ_y) and tensile strength (σ_I) versus sheet thickness for the AA8079 alloy

To determine the specific mechanical properties of the materials, tensile tests were conducted on both the laminate as a whole and its individual layers. In addition to this, an Erichsen cupping test [23] was carried out to determine the material forming depths.

Tensile

In conducting uniaxial tensile tests the elastic and plastic deformation of the layers could be characterized along with the transition between the two types of deformation. For the cold deep drawing of a material it is of great importance to understand the work-hardening effects, the anisotropic behavior and the failure limit of the material [24].

To carry out the testing efficiently a suitable tensile specimen should be used and as the material under study is in the form of thin sheet a flat dog-bone specimen was chosen. The laminate in this case is designed to exhibit high levels of strain at failure and thus a tensile specimen from [25] was deemed appropriate. The specimen is illustrated in Figure 5, with the specific dimensions of [25] labeled. The specimen includes a 25mm gauge length, 6mm gauge width and an 80mm grip-to-grip separation. As the layers are very thin, the determination of strain throughout the test was accomplished by means of a non-contact Zwick/Roell VideoXtens extensometer. The VideoXtens requires that the gauge marks are at a slight angle to the transverse axis of the specimen to allow the marks to be located more easily by the camera.

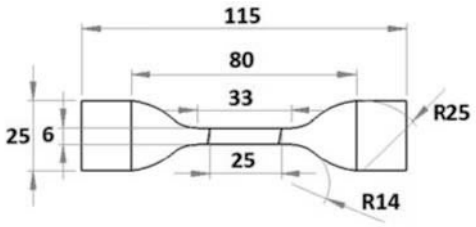

Figure 5 Tensile test specimen, all dimensions in mm

In determining the elastic modulus, and the yield and tensile strengths the engineering stress (σ) – strain (ε) graphs are used. To then determine the strain-hardening exponent (*n*) it is necessary to plot the true stress (s) – strain (e) curves. For a material with uniform deformation in the gauge *n* is determined by conventional true stress-strain techniques, as in Equations 1 -3 [19], [26], where *n* is the slope of the log-log plot of the true stress-strain curve and C is the intercept of the line [19].

$$s = \sigma(1+\varepsilon) \quad (1)$$

$$e = \ln(1+\varepsilon) \quad (2)$$

$$s = Ce^n \Rightarrow \ln s = \ln C + n \ln e \quad (3)$$

These equations can be applied to the laminate, aluminium and PA but due to the localized necking behavior of PVC other methods have to be adopted. Possible methods have been studied previously such as the Gaussian model in Equation (4) [8], [11], where Y is the yield stress, λ is the extension ratio l/l_0, and K is the strain hardening modulus. On occasion it may be appropriate to select a small volume of the material under testing for which uniform deformation can be assumed but there is also potential for issues with the strain softening and strain hardening overlapping [9]. For PVC however it has been observed on occasion that the strain softening can disappear at low strain levels of ~ λ=1.2 [11]

$$\sigma_{True} = Y + K(\lambda^2 - 1/\lambda^2) \quad (4)$$

Normal anisotropy of the layers was measured using Equations 5 and 6. Generally the anisotropy is calculated using the width and thickness of a specimen but measuring the thickness can be troublesome so the length can be used instead by adjusting the equations accordingly [19], [24]. The anisotropy is usually calculated at a strain of 10, 15 or 20% [24].

$$r = (r_0 + r_{90} + 2r_{45})/4 \quad (5)$$

$$r_\infty = \varepsilon_w/\varepsilon_l = [\ln(b/b_o)]/[\ln(l_o b_o/lb)] \quad (6)$$

Finally the Poisson's ratio was calculated as the ratio of lateral strain ε_y against axial strain ε_x given in Equation 7, and the strain sensitivity ($\dot{\varepsilon}$) was determined by analysing the tensile strength of the laminate against the strain rate. The tensile strength was

chosen for the determination of ($\dot{\varepsilon}$) as the failure of the material is of greater interest in cold forming than the yield strength.

$$\nu = -\varepsilon_y/\varepsilon_x \quad (7)$$

Erichsen Test

The Erichsen test is a simple forming limit test designed for metallic sheets [23]. The forming depths of the laminate and the three layers were all determined using the tooling illustrated in Figure 6, where the forming limit is denoted by the Erichsen Index (IE). It must be noted that minor deviations to the test method had to be made such as (i) the maximum blank holding force of the machine being used was 8kN while the standard specifies 10kN, (ii) the safety requirements of the machine did not allow for close observation of the test so a series of samples were tested interpolating between forming depths until the depth at failure was found, and (iii) the punch was made from PTFE where its self-lubricating properties [7] were utilised rather than using graphite grease. The latter deviation was due to the extensive use of PTFE punches in cold forming of the laminate in the pharmaceutical packaging industry.

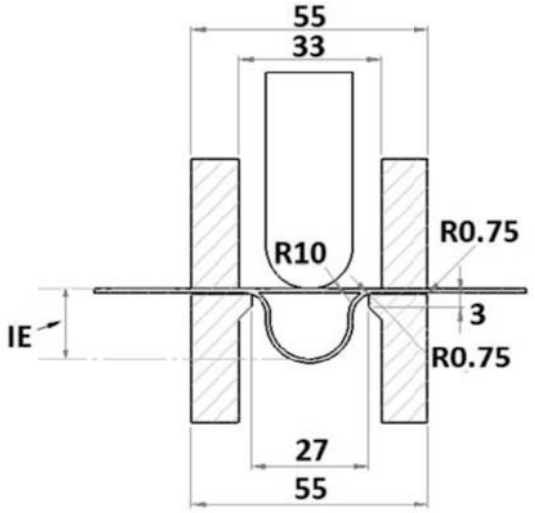

Figure 6 Erichsen test tool with blank in undeformed and deformed shapes and Erichsen Index (IE)

Results

Illustrated in Figure 7 are typical engineering stress - strain curves for each of the three layers and the laminate as a whole. These curves were determined using various strain rates, but as the strain rate increases the accuracy of results decreases. This is due to the sampling rate of the extensometer eventually reaching a maximum and becoming unable to satisfactorily plot a smooth curve above this rate. For this reason the lowest strain rate of $0.0025s^{-1}$ is used to understand the fundamental properties and interactions of the layers.

The foremost property of the materials being tested is the Young's Modulus (E). E was determined for each of the four samples, with the values for the polymer layers given in Table II. In determining the Young's Modulus for the aluminium layer issues arose, with the result deviating from the inherent value of ~70GPa [19]. The Young's modulus in fact tended to vary slightly from one sample to the next, with values of approximately 30GPa being obtained most often. As Young's modulus is an intrinsic property of a given material it is thought that the deviation in this case is as a result of grain size effects [21], [22] and possible surface defects on the samples. The Young's modulus for the laminate has been determined also, but the accuracy of this value is uncertain and will have to be reevaluated once more certainty is gained as regards E for the aluminium.

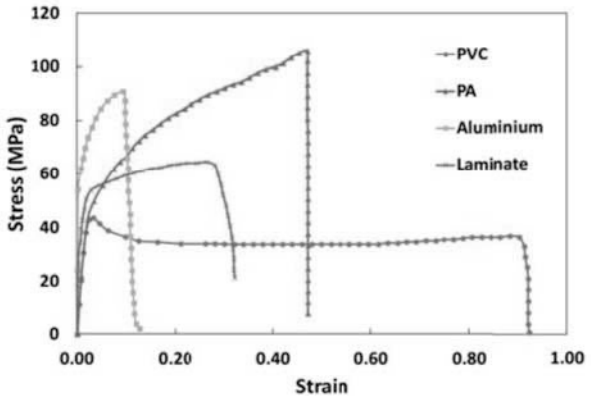

Figure 7 Engineering stress-strain plots for each of the layers and the laminate as a whole

From initial observation on the plasticity of the layers on the other hand, it is evident that the strain-to-failure for both the PA and PVC far exceed that of the aluminium, as expected. The strain-to-failure of the laminate is thus greater than that of the aluminium by a factor of 3. The yield strengths for each layer are similar, indicated in Table II, and thus the yield strength of the laminate is also comparable. The tensile strength on the other hand is strongly influenced by that of the PVC. When the stress-strain curves for the laminate are determined the cross-sectional area used is that of the entire laminate, i.e. thickness of 137μm, but a large proportion of this is the thickness of the PVC which has the highest strain-to-failure ratio. This in addition to the assumption of perfect bonding of the layers [4] could indicate the reduction in tensile strength of the laminate compared to that of the aluminium.

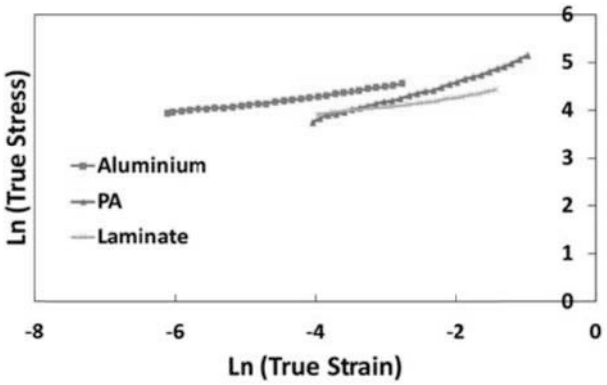

Figure 8 Log-log plots of true stress against true strain, where the slope n is the strain hardening exponent for the given material

The strain hardening of the aluminium and PA is evident in the laminate, without any noticeable contribution by the PVC. Up to the failure strain for the laminate, the PVC exhibits

only strain softening followed by a plateau stress. The minor strain-hardening of the PVC occurs at strains significantly higher than the failure of the laminate, thus having no obvious effect on the laminate properties. The strain hardening curves derived from Equation 3 are illustrated in Figure 8 and their respective slopes given in Table II. The strain hardening curve for PVC is not illustrated due to the issues with determining its true stress – strain curve previously discussed [8], [11]. It is also of interest to note that the assumption of perfect bonding of the layers is strengthened by the observation that there is no localized necking of the PVC layer at yielding, which would occur if the adhesive bond strength was not sufficient.

Table II Yield and tensile strengths for the layers, along with their respective strain-hardening exponents

	Aluminium	PA	PVC	Laminate
E (GPa)	-	2.74	2.36	-
Yield (MPa)	56.43	43.39	49.06	49.65
UTS (MPa)	91.20	110.75	44.78	66.33
n	0.25	0.42	-	0.21
v	0.26	-	-	0.29
r	0.47			0.63

Table III Strains at failure for different angles to the rolling direction of the laminate and aluminium

	0°	45°	90°
Laminate	0.282	0.360	0.275
Aluminium	0.090	0.110	0.081
PA	0.46	-	0.36
PVC	1.07	-	-

As the laminate approaches failure, there is no significant necking present. It has a tendency to fail rapidly once the UTS is reached, with the strains to failure listed in Table III. The strains for 0°, 45° and 90° to the rolling direction are listed, along with those for the aluminium. It is apparent that the strain to failure is higher in the 45° direction, indicating anisotropy of the aluminium, which is evident in the laminate also. The normal anisotropy parameter (r) is given in Table II for both the aluminium and the laminate. The values for both samples differ, which indicates there may be some influence of the polymer layers on the anisotropy. The normal anisotropy is used to give a reasonably good approximation to the limiting drawing ratio of a material [19].

After the tensile specimens fail there is significant elastic recovery of the laminate in the rolled direction, with the specimens curling up tightly on the PA side of the laminate and out to the side of the specimen for the 90° direction. This is thought to be due to bending forces discussed previously [4], but to try and quantify this behavior the PA was tested in both the 0° and 90° directions, resulting in the curves in Figure 9. It is clearly evident that there is more strain-hardening of the PA in the 90° direction (n = 0.62 as opposed to n = 0.42 for 0°), explaining the curling and recovery for 0°. This characteristic could have a significant effect when cold-forming the laminate and in springback of the formed pocket. When these tests were being carried out the temperature and humidity were recorded for future reference, due to the water absorption tendencies of the PA, but the prior history of the PA is unknown and previous conditions may not have been suitable to prevent excessive water absorption.

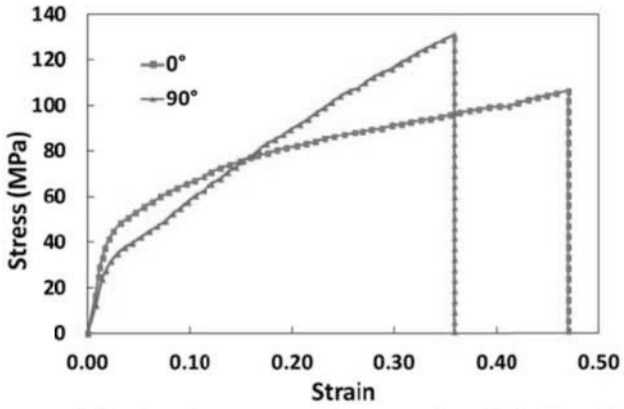

Figure 9 Engineering stress-strain curves for rolled (0°) and transverse (90°) directions of PA

As the laminate is used in a high speed forming process it is of interest to establish the strain rate sensitivity of the laminate, with a number of strain rates ($\dot{\varepsilon}$) tested (0.0025, 0.025, 0.0505, 0.101 and 0.2525s^{-1}). Currently the laminate is formed with a punch speed of 7000mm/min which corresponds to $\dot{\varepsilon}$=4.667s^{-1}, but it was found that no great variation existed in the failure strain above 0.025s^{-1} with a minor increase of 1-2MPa in the tensile strengths of the laminate and aluminum, from one $\dot{\varepsilon}$ to the next. It is important to carry out a strain rate sensitivity test to determine whether a low cycle time would be of significant importance in the formability of the laminate.

Finally, the Erichsen cupping test was conducted, with a trend in the results similar to that for the strain-to-failure of the different layers, as in Figure 7. The tests were carried out three times for each of the four specimens, and were carried out in random order. This randomization was introduced to avoid any errors associated with the test environment, inhomogeneities in the materials and in particular any wear of the PTFE punch during forming. The maximum forming depths without failure are collated in Table IV.

Table IV Erichsen cupping test forming depths (mm)

	Laminate	Aluminium	PA	PVC
Forming Depth (mm)	11.95	7.113	13.907	18.407

Discussion and Conclusions

In conducting this study it was hoped that an insight would be attained into the formability of the laminate and how each of the layers contribute to this formability. Initial analysis was carried out to determine how each of the materials behaves under testing in terms of test environment and pre-treatments. This analysis concluded that significant variation in results can be expected from each of the three layers, in terms of water-absorptivity for PA [7], strain rate and thermal pre-treatment for PVC [8], [11] and annealing temperature and sheet thickness for AA8079 [14], [16]. Each of the materials was subject to tensile testing to determine and compare the properties of each.

The aluminium alloy exhibits good strain-to-failure compared to that for conventional aluminium alloys, with this formability extended considerably by laminating it with polymer layers. The tensile strength of the laminate is lower than that for the aluminium layer, which allows for lower forming forces needed during cold deep drawing of the laminate than would be needed for an aluminium layer of equivalent thickness. The yield and tensile strengths and the plasticity of the aluminium layer also correlate well with previous studies [14], [16]. It was observed that the plasticity determined during testing correlated to a high annealing temperature of ~300°C in Figure 3. This then strengthens the idea of grain-refinement contributing to the formability of the alloy.

The elongation-to-failure of this aluminium layer is enhanced by the addition of the polymer layers. The polymers possess greater elongation-to-failure than the aluminium on its own, and due to exceptional bond strength between the layers the high elongation attributes of the polymers are attained by the aluminium. Anisotropy and strain hardening are evident in the laminate, which can be detrimental to the cold deep drawing and stretching of the laminate, thus the need to quantify them. The multiaxial stretching of the laminate was also tested by means of the Erichsen test and good correlation between these results and those from the tensile tests exist.

As the storage and transport environments of the laminate and layers is not precisely known, the exceptional properties of the laminate could in fact be greater than found here, through stringent control of the storage and forming environments. If excessive moisture absorption of the PA and rapid quenching of the PVC were controlled the maximum formability of the laminate could be determined. The results in this case though are deemed to be representative of those expected in industry as aging and water absorption of the layers is inevitable over time.

References

[1] D. A. Dean, *Pharmaceutical Packaging Technology*. Taylor & Francis, 2000

[2] M. Weiss et al, *Journal of Engineering Materials and Technology*, vol. 129, no. 4, p. 530, 2007

[3] Alcan Packaging University, *Cold Formable High Barrier Laminates,* Überlingen, 5th-6th March 2008

[4] R. M. Jones, *Buckling of Bars, Plates, and Shells*. Bull Ridge Corporation, 2006

[5] Z. Hashin, Journal of Applied Mechanics, Vol. 50, pp. 481-505, Sept. 1983

[6] P. Iaccarino, A. Langella, and G. Caprino, *Composites Science and Technology*, vol. 67, no. 9, pp. 1784–1793, Jul. 2007

[7] R. ZHAO et al, *Transactions of Nonferrous Metals Society of China*, vol. 16, pp. s498–s503, 2006

[8] A. Cross and R. N. Haward, *Polymer*, vol. 19, no. 6, pp. 677–682, 1978

[9] K. Chen and K. S. Schweizer, *Macromolecules*, vol. 44, no. 10, pp. 3988–4000, May 2011

[10] R. N. Haward, *Polymer*, vol. 28, no. 9, pp. 1485–1488, 1987

[11] R. N. Haward, *Macromolecules*, vol. 26, no. 22, pp. 5860–5869, 1993

[12] A. Cross et al, *Polymer*, vol. 20, no. 3, pp. 288–294, 1979

[13] A. S. M. International, *Characterization and Failure Analysis of Plastics*. ASM International, 2003

[14] K. Delijić and D. Radonjić, "The Mechanical Properties and Corrosion Behavior of an Al-Fe-Si (AA8079) Twin Roll Cast Foil", *2nd International Conference on: Deformation Processing and Structure of Materials,* Belgrade, May 2005

[15] B07 Committee, "Specification for Annealed Aluminum and Aluminum-Alloy Foil for Flexible Barrier, Food Contact, and Other Applications," ASTM International, 2006

[16] M. Aghaie-Khafri and R. Mahmudi, *JOM Journal of the Minerals, Metals and Materials Society*, vol. 50, no. 11, pp. 50–52, 1998

[17] R. Mahmudi, *Scripta Metallurgica et Materialia*, vol. 32, no. 12, pp. 2061–2065, Jun. 1995

[18] H. Wielage et al, *Journal of Materials Processing Technology*, vol. 212, no. 3, pp. 685–688, Mar. 2012

[19] S. Kalpakjian and S. Schmid, *Manufacturing, Engineering & Technology*, 5th ed. Prentice Hall, 2005

[20] E04 Committee, "Test Methods for Determining Average Grain Size," ASTM International, 2010

[21] P. J. M. Janssen et al, *Materials Science and Engineering: A*, vol. 419, no. 1–2, pp. 238–248, Mar. 2006

[22] H. S. Kim and M. B. Bush, *Nanostructured Materials*, vol. 11, no. 3, pp. 361–367, May 1999

[23] Erichsen Cupping Test, BS EN ISO 20482, 2003

[24] C. O. Osueke et al, *International Journal of Advanced Engineering Sciences and Technologies,* IJAEST, Vol 9, NO. 2, pp. 280-288, 2011

[25] Plastics - Determination of Tensile Properties, BS EN ISO 527-3, 1996

[26] P. Han, *Tensile testing*. Asm Intl, 1992